CONF-860914--36

A RAPID, SEMIEMPIRICAL METHOD OF CALCULATING THE STABILITY MARGINS OF SUPERCONDUCTORS COOLED WITH SUBCOOLED HE-II

Lawrence Dresner
Oak Ridge National Laboratory*
Oak Ridge, TN 37831

CONF-860914--36

DE88 007264

Abstract

A rapid, semiempirical method is presented for calculating the stability margins of superconductors cooled with subcooled He-II. Based on a model of Seyfert et al.,[1] the method takes into account both time-dependent Gorter-Mellink heat transport and the effects of interfacial Kapitza resistance. The method has been compared favorably with heat transfer data of Seyfert et al.,[1] stability data of Meuris,[2] and stability data of Pfotenhauer and van Sciver.[3]

Introduction

Consider a He-II-cooled superconductor normalized by a sudden heat pulse E, following which it produces a steady Joule power q_J (see Fig. 1). (The symbols are defined in a list at the end of the paper. The quantities E and q_J are normalized to unit area of wetted surface and thus have units J m^{-2} and W m^{-2}, respectively.) What is the maximum value of E that still allows recovery of the superconducting state?

Seyfert et al.[1] have proposed a model by which this maximum value may be calculated. They assume the normalizing pulse causes a phase transition at the wetted surface (burnout) and describe their model in these words: "At the onset of burnout, formation of the thermal barrier starts. The He-II near the heated surface experiences a phase transition. A He-II-He-I interface appears which has its temperature locked at T_λ . . . . We assumed that this barrier had a negligible thickness and that it only affected heat transport in He-II by the condition of a constant temperature, i.e., $T = T_\lambda$, at the hot end of the channels in our test section."

If we assume constant thermophysical properties, we can carry out the calculations required by this model and obtain simple formulas for E.[4] The thermophysical properties that must be assumed constant are the Gorter-Mellink conductivity K (W $m^{-5/3}$ $K^{-1/3}$) and the volumetric heat capacity $S = \rho c_p$ (J m^{-3} K^{-1}). In

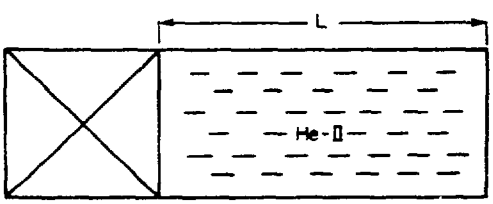

Figure 1. Schematic diagram of a superconductor cooled by contact with a closed He-II-filled channel of length L.

*Oak Ridge National Laboratory is operated by Martin Marietta Energy Systems, Inc., under contract DE-AC05-84OR21400 with the U.S. Department of Energy. Research sponsored by the Office of Fusion Energy, USDOE, and performed while the author was on assignment to the Applied Superconductivity Center, University of Wisconsin, Madison.

Manuscript received September 30, 1986.

actual fact, both vary strongly with temperature, especially near T_λ, so we cannot expect the formulas for E to have more than order-of-magnitude accuracy. However, there are several experimental measurements[1,2] of E that can be used to correct the theoretical formulas and thus convert them into the rapid method of calculation advertised in the title.

Method of Calculation

If the normal-state Joule power q_J is large enough, recovery must take place before much heat has reached the distal end of the cooling channel. In this case, the channel looks, from the proximal end, like an infinitely long channel. Seyfert's model then gives

$$E = \frac{1}{4} K^3 S\,(T_\lambda - T_b)^2\, q_J^{-3}\ . \qquad (1)$$

On the other hand, when q_J is small enough,

$$E = E_o \equiv [h(T_\lambda) - h(T_b)]\, L \qquad (2)$$

where h is the enthalpy per unit volume of helium. If we plot E/E_o as ordinate and q_J/q_* as abscissa, where

$$q_* = \frac{(K^3 S)^{1/3}\,(T_\lambda - T_b)^{2/3}}{(4E_o)^{1/3}}\ , \qquad (3)$$

we find from (1) and (2) that

$$\frac{E}{E_o} = \begin{cases} 1 , & q_J/q_* \ll 1 \qquad (4a) \\ (q_J/q_*)^{-3} , & q_J/q_* \gg 1 \qquad (4b) \end{cases}$$

These two limits are shown in Fig. 2 together with ten experimental points reported by Meuris,[2] five for T_b = 2.0 K and five for T_b = 2.1 K. Meuris' points have been made to fit the high-flux limit (4b) by appropriately choosing $KS^{1/3}$. Table 1 gives the best-fit values together with the point values referring to the sample temperature. The points of Seyfert et al.,[1] not shown in Fig. 2, all lie on the limit (4b), which they have been made to fit in ref. 4 also by appropriately choosing $KS^{1/3}$.

The ratio in the fourth column of Table 1 varies fairly smoothly with $T_\lambda - T_b$, as shown in Fig. 3. Applying this correction factor to the point data for $KS^{1/3}$, we can rapidly estimate E as a function of q_J with the universal curve of Fig. 2. The ratio of the best fit to the point values of $KS^{1/3}$ varies roughly with T_b as $1.3(T_\lambda - T_b)^{0.6}$.

The Kapitza Limit

The high-flux limit (4b) for E cannot be valid for arbitrarily large Joule powers q_J. For if q_J is large enough, the temperature difference across the phase boundary induced by the Kapitza resistance will be

Table 1. Comparison of Best-Fit and Point Values of $KS^{1/3}$

T_b (K)	$KS^{1/3}$ (best-fit) ($W^{4/3}$ $cm^{-8/3}$ $s^{1/3}$ $K^{-2/3}$)	$KS^{1/3}$ (point) ($W^{4/3}$ $cm^{-8/3}$ $s^{1/3}$ $K^{-2/3}$)	Ratio (best-fit/point)	Experiment
1.8	5.68	7.73	0.735	Seyfert et al., ref. 1
1.9	5.68	9.52	0.596	Seyfert et al., ref. 1
2.0	3.68	10.6	0.347	Meuris, ref. 2
2.1	2.30	8.62	0.267	Meuris, ref. 2

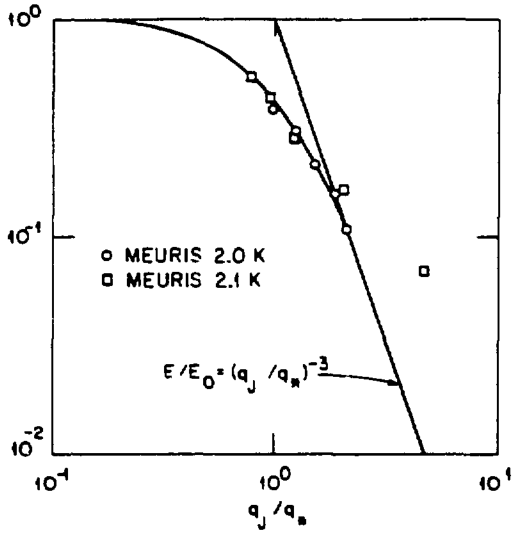

Figure 2. Universal curve of normalized heat pulse E/E_o versus normalized Joule heat flux q_J/q_*.

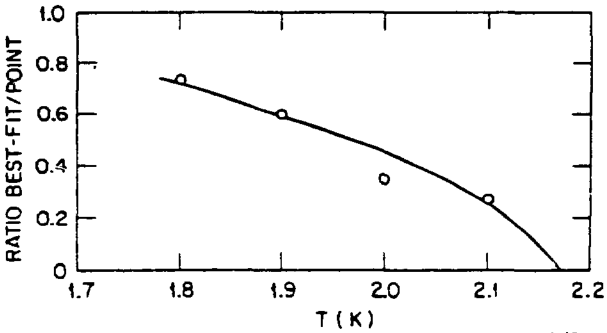

Figure 3. Ratio of best fit to point values of $KS^{1/3}$ versus ambient helium temperature T_b. The points are from Table 1; the curve is the equation $1.3(T_\lambda - T_b)^{0.6}$.

large enough to keep the metal temperature T_m above the current-sharing threshold. When this happens the curves of Kapitza flux

$$q_K = a(T_m^n - T_{He}^n) \tag{5}$$

and the Joule power q_J plotted against metal temperature T_m intersect as shown in Fig. 4a, and recovery is never possible. For small enough q_J, q_K always lies above q_J, and recovery is always possible. The limiting case occurs when q_K and q_J touch at only one point; this can happen in two different ways, as shown in Figs. 4b and 4c.

What criterion distinguishes alternative 4b from alternative 4c? The temperature T_o of tangency in Fig. 4c is determined by the conditions

$$\frac{q_K}{T_o - T_{cs}} = \frac{q_{J\,max}}{T_{cr} - T_{cs}} = \left(\frac{dq_K}{dT}\right)_{T_o} . \tag{6}$$

If $T_m^n >> T_{He}^n$, as is usually true, we can ignore the second term in the expression for q_K and take q_K to be aT_m^n. Then (6) gives

$$T_o = \frac{n}{n-1} T_{cs} , \tag{7a}$$

and

$$q_K = \frac{q_{J\,max}}{n-1} \frac{T_{cs}}{T_{cr} - T_{cs}} . \tag{7b}$$

The temperature of tangency is larger than T_{cs}; it will be smaller than T_{cr} if

$$i > \frac{T_{cr}}{(T_{cr} - T_b)n} . \tag{7c}$$

The inequality (7c) must be fulfilled for alternative 4c to apply; otherwise alternative 4b holds. So the Kapitza resistance puts the following limits on the Joule power:

$$q_{J\,max} = q_K(T_{cr}) \quad , \; i < \frac{T_{cr}}{(T_{cr} - T_b)n} \tag{8a}$$

$$q_{J\,max} = \frac{(n-1)(T_{cr} - T_{cs})}{T_{cs}} q_K\left(\frac{n}{n-1} T_{cs}\right),$$

$$i > \frac{T_{cr}}{(T_{cr} - T_b)n} . \tag{8b}$$

In a typical one of Meuris' experiments, q_K = 20 W cm^{-2} [B = 8.0 T, T_b = 2.0 K, T_{cr} = 5.6 K, I_T = 1000 A, I_{cr} = 2900 A, i = 0.344, T_{cs} = 4.36 K, RHS of (7c) = 0.389, a = 0.020 W cm^{-2} K^{-4}, n = 4, q_K (T_{cr}) = 19.7 W cm^{-2}]. But $q_{J\,max}$ was at most one-quarter as

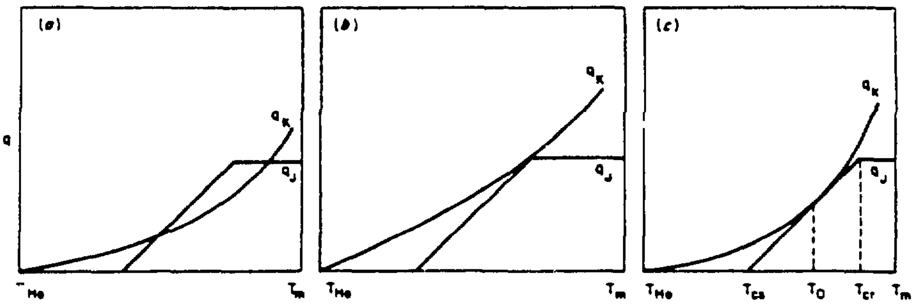

Figure 4. Sketches showing the relation of the Kapitza flux q_K and the Joule power q_J in case of nonrecovery, (a), and in two possible limiting cases, (b) and (c).

large, so the Kapitza limit (8a,b) played no role in Meuris' experiments.

The Two-Dimensional Channel

Pfotenhauer and van Sciver[3] have studied the stability margin of a two-dimensional channel such as that shown schematically in Fig. 5. How might we expect the stability margin E to vary as a function of the Joule power per unit heated surface q_s? When q_s is small, the transverse temperature distribution (transverse means in the x-direction) is nearly uniform, and the channel behaves like a one-dimensional channel in the y-direction of length L and Joule heat flux $q_J = (w/d)q_s$. The stability margin of such a channel is given by the universal curve of Fig. 2, shown in the log-log plot of Fig. 6 spanning the asymptotes $E = E_0 = [h(T_\lambda) - h(T_b)]L$ and $E = Cq_J^{-3}$, $C = K^3 S(T_\lambda - T_b)^2/4$. When q_s is large and $d << w$, the two-dimensional channel behaves like a one-dimensional channel of length d and Joule heat flux $q_s = (d/w)q_J$. The stability margin of such a channel can be represented in Fig. 6 by the universal curve of Fig. 2, this time spanning the asymptotes $E = (d/L)E_0$ and $E = Cq_s^{-3} = C(w/d)^3 q_J^{-3}$. If these two universal curves are faired together, we get the stepped heavy curve that represents how we expect the stability margin of the two-dimensional channel to behave when $d << w$. If $d >> w$, the two-dimensional channel will behave like a one-dimensional channel only for very large q_s when E approaches the asymptote $Cq_s^{-3} = C(w/d)^3 q_J^{-3}$, which now lies to the left of the curve $E = Cq_J^{-3}$. E should depart from this asymptote when it is of the order of $(d/L)E_0$. The unstepped heavy curve represents how we expect the stability margin of the two-dimensional channel to behave when $d >> w$. Finally, we must add the Kapitza limits (8a) or (8b) to Fig. 6.

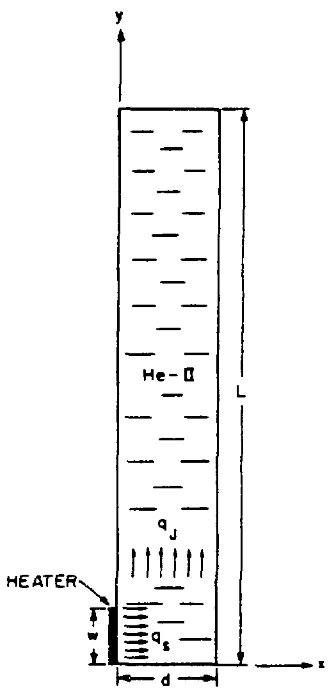

Figure 5. Schematic diagram of a two-dimensional channel filled with He-II. Note the placement of the heater in the side wall.

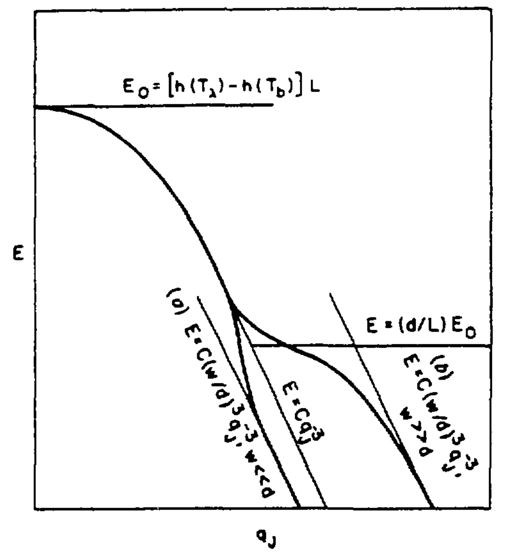

Figure 6. A sketch of the stability margin of the two-dimensional channel as a function of q_J when (a) $w << d$, (b) $w >> d$.

Figure 7 shows Pfotenhauer and van Sciver's experimental points. In their paper, Pfotenhauer and van Sciver noted that the Joule power per unit area did not remain constant during the course of an experiment. They chose to define q_J in a way that caused the

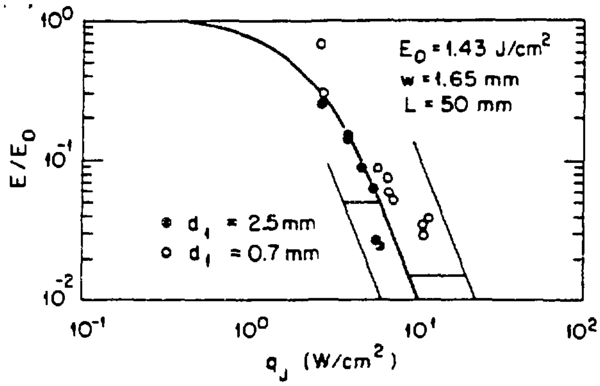

Figure 7. The experimental points of Pfotenhauer and van Sciver (ref. 3) and the various theoretical curves described in the text.

experimental points to lie slightly to the right of the theoretical curve of Fig. 2. In Fig. 7, I have normalized q_J so that the asymptote $E = Cq_J^{-3}$ passes through the cluster of experimental points near $E/E_o = 0.1$. Also shown in Fig. 7 are the asymptotes $E = C(w/d)^3 q_J^{-3}$ for both sets of points and the corresponding values of $E = (d/L)E_o$ (shown as horizontal line segments). Both sets of points seem to behave as described in the previous paragraph.

It might be argued that the sharp drop in the solid points near $q_J = 6$ W/cm^2 signifies approach to the Kapitza limit. The corresponding limit for the open points would be $q_J = (2.5/0.7)6 = 21.4$ W/cm^2. Thus the open points would be unaffected by the Kapitza limit in any case.

References

1. P. Seyfert, J. Lafferranderie, and G. Claudet, "Time-Dependent Heat Transport in Subcooled Superfluid Helium," Cryogenics, 22, 401-408, 1982.

2. C. Meuris, "Experimental Study of the Stability of a Superconductor Cooled by a Limited Volume of Superfluid Helium," IEEE Trans. Magn., MAG-19(3), 272-275, 1983.

3. J. Pfotenhauer and S. W. van Sciver, "Stability Measurements of a Superconductor Cooled by a Two-Dimensional Channel of He-II," Paper DA-4, 1985 CEC/ICMC Conference, Cambridge, Mass., August 12-16, 1985.

4. L. Dresner, "Transient Heat Transfer in Superfluid Helium – Part II," Adv. Cryog. Eng., 29, 323-333, 1984.

List of Symbols

- a proportionality constant in Kapitza's law of interfacial heat transport, Eq 5 [W m^{-2} K^{-n}]
- c_p specific heat at constant pressure [J kg^{-1} K^{-1}]
- C abbreviation for $K^3 S(T_\lambda - T_b)^2/4$
- d width of the two-dimensional channel [m]
- E heat pulse energy per unit area [J m^{-2}]
- E_o available enthalpy of He-II per unit area, cf. Eq 2 [J m^{-2}]
- h enthalpy per unit volume of helium [J m^{-3}]
- i ratio of the transport current to the critical current
- K Gorter-Mellink conductance [W m$^{-5/3}$ K$^{-1/3}$]
- L length of the channel [m]
- n exponent in Kapitza's law of interfacial heat transport, Eq 5
- q_J Joule heat flux down the length of the channel [W m^{-2}]
- q_K Kapitza heat flux, cf. Eq 5 [W m^{-2}]
- q_s Joule power per unit heated surface [W m^{-2}]
- q_* a fiducial heat flux defined by Eq 3 [W m^{-2}]
- S ρc_p, the heat capacity per unit volume [J m^{-3} K^{-1}]
- T temperature [K]
- T_b ambient helium temperature [K]
- T_{cr} critical temperature [K]
- T_{cs} current-sharing threshold temperature [K]
- T_{He} helium temperature [K]
- T_m metal temperature [K]
- T_o temperature of tangency, cf. Fig. 4c [K]
- T_λ the (lambda) temperature of phase change from He-II to He-I [K]
- w the width of the heater in the two-dimensional channel [m]
- ρ density [kg m^{-3}]

DISCLAIMER